DNA Reaction System that Acquires Classical Conditioning

ACS Synthetic Biology

pubs.acs.org/synthbio
Research Article

DNA Reaction System That Acquires Classical Conditioning

Takashi Nakakuki,* Masato Toyonari, Kaori Aso, Keiji Murayama, Hiroyuki Asanuma, and Tom F. A. de Greef

Cite This: ACS Synth. Biol. 2024, 13, 521−529

ABSTRACT: Biochemical reaction networks can exhibit plastic adaptation to alter their functions in response to environmental changes. This capability is derived from the structure and dynamics of the reaction networks and the functionality of the biomolecule. This plastic adaptation in biochemical reaction systems is essentially related to memory and learning capabilities, which have been studied in DNA computing applications for the past decade. However, designing DNA reaction systems with memory and learning capabilities using the dynamic properties of biochemical reactions remains challenging. In this study, we propose a basic DNA reaction system design that acquires classical conditioning, a phenomenon underlying memory and learning, as a typical learning task. Our design is based on a simple mechanism of five DNA strand displacement reactions and two degradative reactions. The proposed DNA circuit can acquire or lose a new function under specific conditions, depending on the input history formed by repetitive stimuli, by exploiting the dynamic properties of biochemical reactions induced by different input timings.

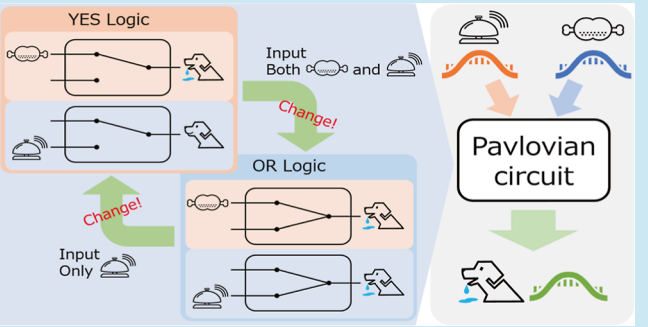

KEYWORDS: *classical conditioning, learning, memory, forgetting, DNA strand displacement*

INTRODUCTION

It has recently become possible to construct biochemical reaction systems with intrinsic plastic adaptation capabilities by rationally combining existing basic reaction mechanisms.[1−3] This capability is based on the versatility of biomolecules, such as proteins,[4] and the structure and dynamics of biochemical reaction systems.[5] The principles underlying the plastic adaptability of biochemical reaction systems to their environment represent a crucial issue in academic fields dealing with biochemical reaction systems beyond systems biology.[6]

Recent advances in DNA nanotechnology have enabled methodologies to explore the operating principles of biochemical reaction systems with artificially synthesized nucleic acids to construct specific biomolecular reaction networks.[7] Systems with plastic adaptation have memory and learning capabilities and have been actively studied in the field of DNA computing over the past decade,[8−11] as pioneered by Qian et al.[12] These studies focus primarily on implementing well-established machine learning algorithms, such as neural networks, on DNA reaction systems (hereafter, DNA circuits), while addressing basic learning at the simulation level.[13] In contrast, an operating principle that can alter the circuit functions depending on the history (stimulus level and timing) of the input stimuli while considering the dynamic properties of DNA circuits has been proposed,[14,15] implying further possibilities to extend the capability of biochemical reaction systems.[16−20] However, adaption to DNA circuits with memory and learning capabilities by exploiting the dynamic properties of biochemical reactions remains challenging.[21]

Based on the importance of understanding the operating principles of biochemical reaction systems with intrinsic plastic adaptation capabilities, we aimed to develop a DNA circuit with memory and learning capabilities. In this study, a DNA circuit that acquires classical conditioning as a typical learning task was considered using a simple reaction mechanism in an experimentally feasible manner. Classical conditioning, also known as Pavlovian conditioning,[22] is a physiological phenomenon based on memory and learning in which the paired presentation of stimuli results in associations between the elements and changes in response. By extending the design concept and fully utilizing the dynamic properties of biochemical reaction systems induced by different input timings,[15] we constructed a basic DNA circuit that can plastically acquire or forget new functions under a specific condition, depending on the input history formed by repetitive stimuli.

Received: July 26, 2023
Revised: January 10, 2024
Accepted: January 11, 2024
Published: January 27, 2024

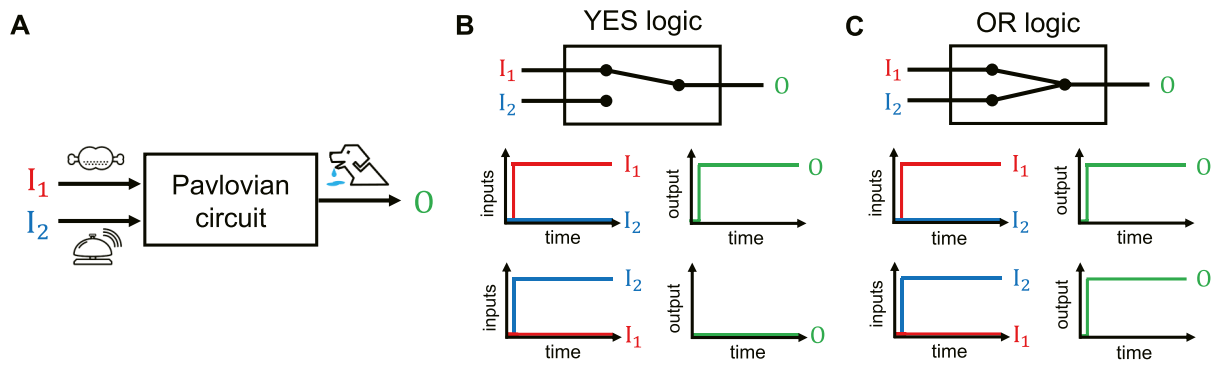

Figure 1. Conditioned reflex circuit. (A) Conditioned reflex circuit is a logical circuit with two inputs, I_1 and I_2, and an output, O. (B) In the prelearning condition, the circuit functions as a "YES" gate, where the output O responds to only I_1 but not to I_2. (C) In the postlearning condition, the circuit functions as an "OR" gate, where the output O responds not only to I_1 but also to I_2.

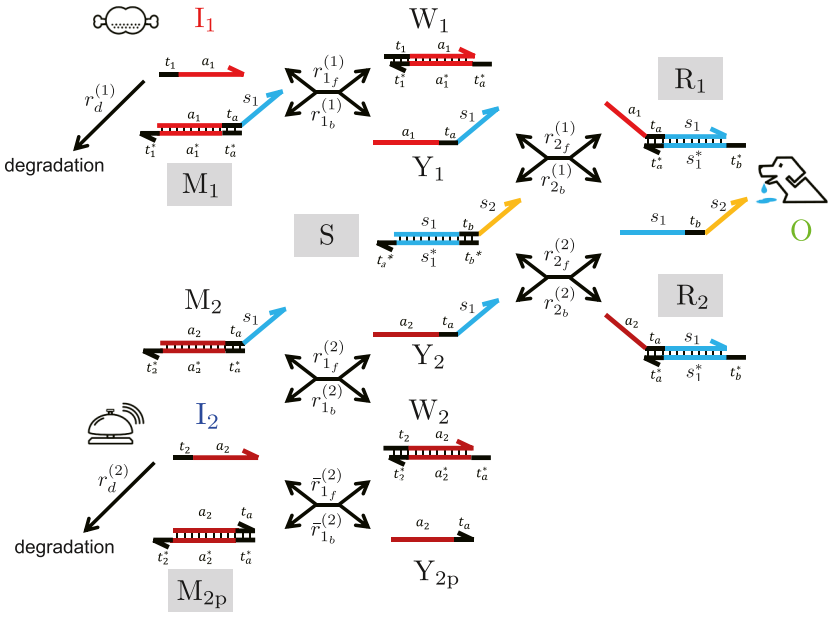

Figure 2. Schematic view of the conditioned reflex circuit using the DNA strand displacement mechanism. The reactions are described with six single-stranded DNAs (I_1, I_2, Y_1, Y_2, Y_{2p}, and O) and eight double-stranded DNAs (M_1, M_2, M_{2p}, W_1, W_2, S, R_1, and R_2). Their structures are illustrated with directional arrows; the arrowhead denotes the 3′ end, and the opposite side is the 5′ end. Each DNA strand comprises some domains, where the labels t_1, t_2, t_a, and t_b are the toehold domains that provide the starting point of the binding in the DNA strand displacement reaction, and the labels a_1, a_2, s_1, and s_2 are the recognition domains that control the linkage of the binding reaction. A double-stranded DNA is illustrated by two opposing arrows with hatching, and domains that have complementary base sequences are indicated by an asterisk (e.g., t_1* and s_1*). The bidirectional arrows connecting the DNA strands denote reversible DNA strand displacement reactions ($r_{1_f}^{(1)}$, $r_{1_b}^{(1)}$, $r_{1_f}^{(2)}$, $r_{1_f}^{(2)}$, $\overline{r}_{1_f}^{(2)}$, $\overline{r}_{1_b}^{(2)}$, $r_{2_f}^{(1)}$, $r_{2_b}^{(1)}$, $r_{2_f}^{(2)}$, and $r_{2_b}^{(2)}$), where the forward and backward reactions are denoted by subscript "f" and "b", respectively, and the directional arrows from I_1 and I_2 denote the degradation reactions ($r_d^{(1)}$ and $r_d^{(2)}$). The double-stranded DNAs that have initial concentrations at the prelearning condition are denoted by shadowed, square boxes.

RESULTS AND DISCUSSION

Circuit Design. The Pavlovian-conditioned reflex is a typical example of classical conditioning.[22] When food is presented to a dog, the dog unconsciously secretes saliva as a result of a physiological phenomenon known as "unconditioned reflex." In contrast, ringing a bell without presenting food to the dog does not trigger the unconditioned reflex. However, by repeating trials of ringing the bell while simultaneously presenting food to the dog, the dog begins to salivate upon mere ringing of the bell. This responsive change is known as "conditioned reflex", a learning mechanism in the brain where food and bells are considered unconditioned and conditioned stimuli, respectively. A recent study elucidated the mechanism of Pavlovian conditioning through a series of murine experiments. In the striatal medium spiny neurons, the transmission efficiency of synaptic (excitatory) signaling with glutamate can plasticly increase at a specific condition, wherein the condition is that reward signaling with dopamine acts on the synaptic signaling within a narrow time window after glutamate activation.[23] Forgetting the acquired conditioned reflex is also an important mechanism for learning systems. After a conditioned reflex has been established, if only the conditioned stimulus is administered repetitively without the unconditioned stimulus, then the conditioned reflex no longer occurs.

https://doi.org/10.1021/acssynbio.3c00459
ACS Synth. Biol. 2024, 13, 521−529

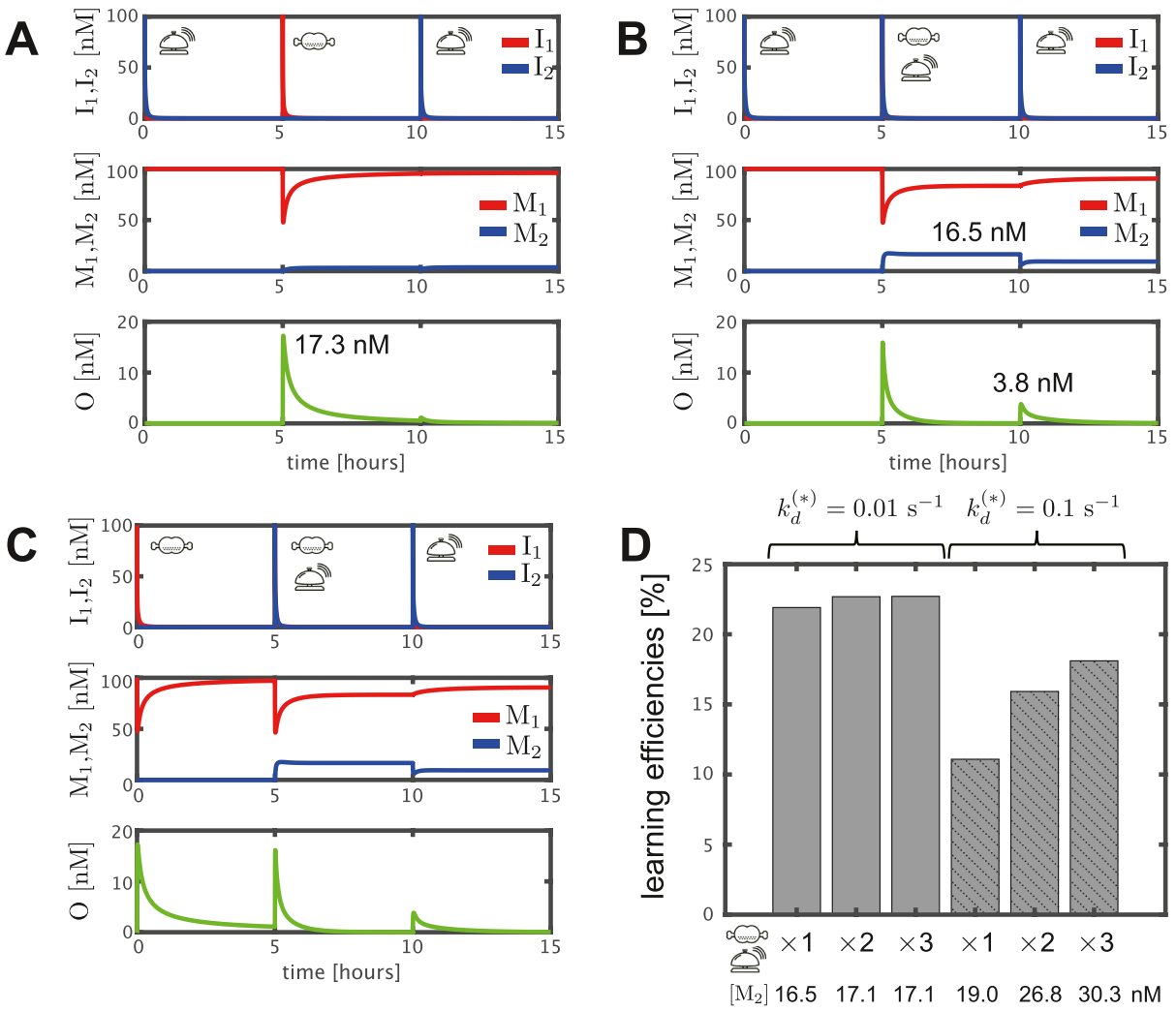

Figure 3. Acquiring conditioned reflexes depending on input patterns. (A−C) The upper, middle, and lower panels show the time-course data of inputs, memory gates, and outputs, respectively. The input patterns are "B−F−B" for (A), "B−FB−B" for (B), and "F−FB−B" for (C). The peak values of interest are denoted in the lower panels of (A,B). (D) Learning efficiencies are calculated by the peak of the I_2-induced output in the postlearning condition divided by the I_1-induced output in the prelearning condition, where the I_2-induced outputs after one, two, and three repetitive, simultaneous inputs were evaluated in two different parameter settings. The accumulated concentrations of M_2 for input patterns "FB", "FB−FB", and "FB−FB−FB" are denoted below the plot. The detailed data are also shown in Figures S6 and S7.

The learning mechanism in Pavlovian conditioning can be simplified from the perspective of logical operations as follows: consider a two-input and one-output circuit, as shown in Figure 1A, where I_1 and I_2 conceptually correspond to "feed-related" and "bell-related" inputs and O "saliva" output, respectively. In the prelearning unconditional reflection, the circuit function corresponds to "YES" logic that outputs only in response to input I_1 but not to I_2 (Figure 1B). However, via the learning process in which repeated simultaneous inputs of both I_1 and I_2 are provided, in the postlearning conditional reflection, the circuit function alters to "OR" logic that responds not only to I_1 but also to I_2 (Figure 1C). Nonetheless, if only input I_2 is repeatedly applied in the postlearning condition, the output responses to I_2 gradually weaken; that is, the OR function is gradually lost toward the YES circuit. In this study, we define this plastic, changeable circuit as a "conditioned reflex circuit."

In accordance with the abstracted operation of classical conditioning, we designed the conditioned reflex circuit based on a toehold-mediated DNA strand displacement mechanism (Figure 2), where the chart drawn by Visual DSD[24] is also provided in Figure S1. The operation principle is summarized as follows:

Operation in the Prelearning Condition (Unconditional Reflection). In the case that only input strand I_1 is provided (Figure S2A), the first-round strand displacement reaction ($r_{1_f}^{(1)}$ and $r_{1_b}^{(1)}$) triggered by the binding of I_1 with memory gate M_1 generates an excitation strand Y_1 and waiting strand W_1. Subsequently, the second-round strand displacement reaction ($r_{2_f}^{(1)}$ and $r_{2_b}^{(1)}$), triggered by the binding of Y_1 with reservoir gate S, generates an output strand O and reward strand R_1. Notably, output O also induces a different strand displacement reaction ($r_{2_b}^{(2)}$ and $r_{2_f}^{(2)}$) with reward strand R_2 simultaneously while generating excitation strand Y_2. In contrast, in the case that only the input strand I_2 is provided (Figure S2B), the first-round strand displacement reaction ($r_{1_f}^{(2)}$ and $r_{1_b}^{(2)}$) does not occur as long as M_2 has no initial concentration. Instead,

https://doi.org/10.1021/acssynbio.3c00459
ACS Synth. Biol. 2024, 13, 521−529

another first-round strand displacement reaction ($\overline{r}_{1_f}^{(2)}$ and $\overline{r}_{1_b}^{(2)}$) between I_2 and pseudomemory gate M_{2p} occurs while generating the pseudoexcitation strand Y_{2p} and waiting strand W_2.

Operation during the Learning Process. In a case where I_1 and I_2 are provided simultaneously (Figure S2C), all strand displacement reactions occur as explained above. Subsequently, it follows a special condition for learning that Y_2 and W_2 appear simultaneously, and consequently, the strand displacement reaction $r_{1_b}^{(2)}$ triggered by the binding of Y_2 with W_2 updates the memory gate concentration M_2.

Operation in the Postlearning Condition (Conditional Reflection). In the postlearning condition, we assume that a sufficient initial concentration is stored in M_2. On top of the output response by input I_1 as with the prelearning condition, even in the case that only I_2 is applied, the first- and second-round strand displacement reactions ($r_{1_f}^{(2)}$, $r_{1_b}^{(2)}$, $r_{2_f}^{(2)}$, and $r_{2_b}^{(2)}$) occur with a sufficient amount of M_2, while generating output strand O and reward strand R_2.

Renewable Mechanism for Responding to Repetitive Inputs. For the learning circuit, a renewable mechanism is essential to respond to repetitive inputs. More precisely, all single- and double-stranded DNAs, except for the memory gate M_2, must return to their initial concentrations after the output response to the previous input in preparation for the next input. As all strand displacement reactions are designed to be reversible, the circuit can be "renewable" by introducing any adequate reaction mechanism ($r_d^{(1)}$ and $r_d^{(2)}$) to eliminate I_1 and I_2, such as a degradation reaction by exonucleases.

Acquiring Conditioned Reflex. We have verified our design of the conditioned reflex circuit based on numerical simulations, where the mathematical model described by ordinary differential equations, the strand displacement reaction rates $k_{i_f}^{(j)}$, $k_{i_b}^{(j)}$, $\overline{k}_{1_f}^{(1)}$, and $\overline{k}_{1_b}^{(1)}$ (i, j = 1, 2), the degradation rates $k_d^{(1)}$ and $k_d^{(2)}$, and initial concentrations are provided in the Methods section. All of the simulations were performed with Matlab (MathWorks, Inc.). First, we evaluated the operation in the prelearning condition (Figure S2D−F). The output responses appeared in the input conditions of ($[I_1](0)$, $[I_2](0)$) = (100, 0) for (D), ($[I_1](0)$, $[I_2](0)$) = (100, 100) for (F), but not ($[I_1](0)$, $[I_2](0)$) = (0, 100) for (E), where $[I^*](0)$ denotes the initial concentration (nM) of strand I^* at t = 0. In addition, the renewable mechanism by degradation reactions $r_d^{(1)}$ and $r_d^{(2)}$ successfully works to restore the concentration distribution in the reaction system after responses to its initial concentrations, except for the desired accumulation of the memory gate M_2 in the learning condition ($[I_1](0)$, $[I_2](0)$) = (100, 100) (also see Figures S3−S5 for the time-course data of all strands). Next, we evaluated the operations when various input patterns were applied to the circuit to confirm that its function is plastically altered only under the learning condition. For the sake of simplicity of notation, we denoted the input pattern, which comprised multiple consecutive inputs in the timeline, by a character string formed by concatenating "F" as "feed-related" I_1 and "B" as "bell-related" I_2. For example, input pattern F−B−F represents three consecutive inputs of I_1, I_2, and I_1 over time. In addition, simultaneous inputs are denoted by "FB." In the case of the input pattern "B−F−B", which does not satisfy the learning condition, the first input I_1 induced a strong output (17.3 nM of peak), but the following input I_2 did not trigger the responses as the concentration of memory gate M_2 was not increased noticeably (Figure 3A). However, in the case of patterns "B−FB−B", which satisfy the learning condition, although the first-time I_2 did not trigger the response, the second-time I_2 successfully induced the output response (3.8 nM of peak) as the simultaneous inputs I_1 and I_2 led to an increase in M_2 concentration (16.5 nM) during the period of resetting (Figure 3B). Other learning conditions, such as "F−FB−B" also induced a reasonable "update" of memory gate M_2 (Figure 3C). In terms of learning efficiency, the peak of the I_2-induced output in the postlearning condition was approximately 22.0% (=3.8/17.3 × 100) of the I_1-induced output in the prelearning condition, as indicated in Figure 3A,B. In particular, the learning efficiencies were not markedly increased even if several simultaneous inputs were applied to the circuit. This can be explained in terms of the update width of the memory gate M_2, where the accumulated concentrations of M_2 after repetitive "FB" inputs were 16.5, 17.1, and 17.1 nM for input patterns "FB", "FB−FB", and "FB−FB−FB", respectively (Figure 3D). The update width of M_2 is dependent on the gate concentrations and degradation rate. For example, by doubling the gate concentrations ($[M_1](0)$ = $[M_{2p}](0)$ = $[S](0)$ = $[R_2](0)$ = 200 nM) and increasing the degradation rate $k_d^{(*)}$ by a factor of 10, M_2 can be updated from 19.0 to 30.3 nM in a stepwise manner (Figure 3D). It should be noted that the output property of the conditioned reflex circuit can be suitably reprocessed by various methods, depending on the applications. For example, as discussed below, the output amplitude can be considerably enhanced by adding a threshold gate to the circuit.

Forgetting Conditioned Reflex. The conditioned reflex was first acquired by the simultaneous input of I_1 and I_2; then, only the I_2 input was applied nine times repetitively (that is, we applied the input pattern "FB−B−B−B−B−B−B−B−B−B") (Figure 4). The accumulated concentration of M_2 and the output response peaks gradually decreased (Figure S8) as the repetitive I_2 inputs were provided. The speed of forgetting is dependent on gate concentration and degradation rate. In fact,

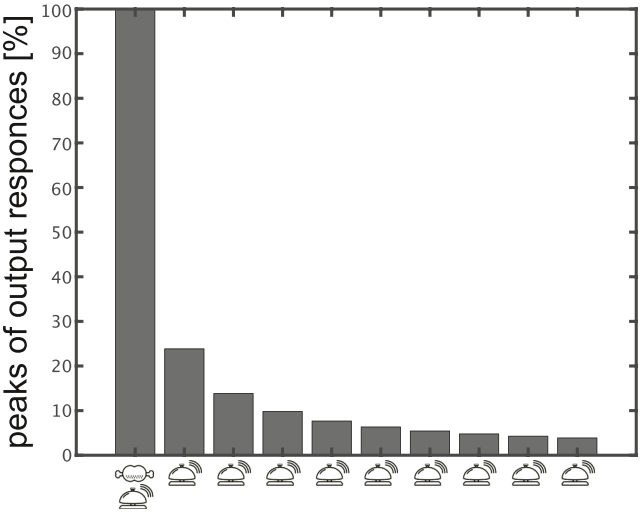

Figure 4. Forgetting the conditioned reflex. The peak of the output response for each input of the input pattern "FB−B−B−B−B−B−B−B−B−B" is calculated, where the peaks are normalized by that of the first "FB" input case. Detailed data are shown in Figure S9.

https://doi.org/10.1021/acssynbio.3c00459
ACS Synth. Biol. 2024, 13, 521−529

a more rapid decrease in peaks of output responses was observed in the circuit with the setting $[M_1](0) = [M_{2p}](0) = [S](0) = [R_2](0) = 200$ nM, $[R_1](0) = 50$ nM, and $k_d^{(1)} = k_d^{(2)} = 0.1\ s^{-1}$ (Figure S10), where the initial dumping of output peak with I_2 input was approximately twice as large.

Generalization of the Conditioned Reflex Circuit. In general, classical conditioning is a learning task defined for multiple-input systems. In this section, we consider extending the two-input conditioned reflex circuit to a multiple-input counterpart. Figure 5 shows a schematic view of a generalized

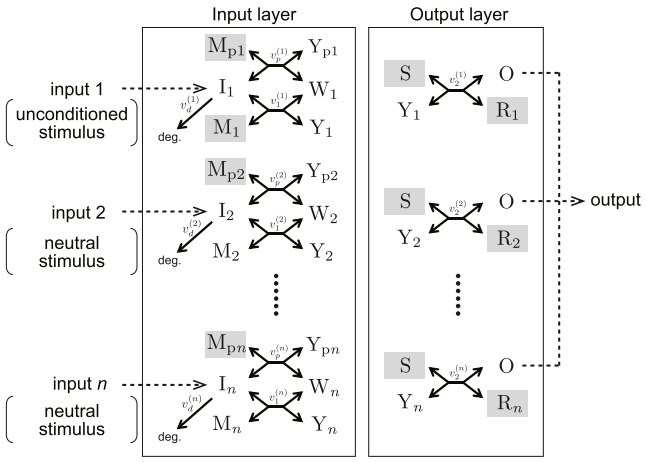

Figure 5. Generalization of the conditioned reflex circuit. Input I_1 is designed as an unconditioned stimulus that induces the output response, and others $I_2,\cdots,I_n$ are designed as neutral stimuli that do not induce the output response in the prelearning condition. The double-stranded DNAs that have initial concentrations at the prelearning condition are denoted by shadowed, square boxes.

version of the conditioned reflex circuit with n-input channels. For simplicity of notation, let a combination of n inputs (I_1, $I_2,\cdots$, I_n) simultaneously applied to the circuit at a certain time be defined by $\mathcal{I} = (i_1, i_2, ..., i_n)$, where i_k is 1 if the input I_k is included in the combination and otherwise 0. For example, if inputs I_1, I_3, and I_n are simultaneously applied to the circuit, we denote the combination of inputs as $\mathcal{I} = (1, 0, 1, 0, ..., 0, 1)$. The learning task for the multiple-input version of classical conditioning is defined as Consider the n-input and 1-output circuit (Figure 5), where the input I_1 and others $I_2,\cdots,I_n$ are designated as the unconditioned stimulus being responsive and neutral stimuli being nonresponsive at the initial state in the prelearning condition, respectively. Assume that two consecutive inputs $\mathcal{I}_1$ and $\mathcal{I}_2$ are applied to the circuit at an appropriate time interval; for the first input $\mathcal{I}_1$, a combination of $I_1,I_{c1},I_{c2},\cdots,I_{cm}$ is employed, where $c_1, c_2, ..., c_m \in \{2, 3, ..., n\}$ ($m \leq n - 1$), and m is a positive integer. Then, the circuit is called a "generalized conditioned reflex circuit" if the output O is responsive only upon $\mathcal{I}_2$ such that at least one of $\{i_1, i_{c1}, i_{c2},\cdots, i_{cm}\}$ is 1 and the others are zero. We performed the numerical experiments on the generalized conditioned reflex circuit with four input channels, for which the mathematical model and the parameters are provided in the Methods section. Since we assume simultaneous inputs with the unconditioned stimulus I_1 for $\mathcal{I}_1$ in prelearning condition, there are eight possible combinations for $\mathcal{I}_1$. According to the output responses for all 32 input histories when only one input was applied for $\mathcal{I}_1$ in the postlearning condition, we can see that the output O was responsive in the case of the 12 input histories that were expected to obtain the conditioned reflex, in addition to the trivial eight input histories shown in the first column (Figure S11). We also confirmed that simulations of all 120 possible input histories, including the 32 cases, agreed with the expected results (Figure S12). Since the generalized conditioned reflex circuit consists of a minimal number of reaction mechanisms, the learning efficiency tends to decrease as the number of input channels increases (See Figure S13 for the 10-input case). However, the dynamic behaviors qualitatively demonstrate that the conditioned reflexes were acquired by this minimal mechanism.

Discussion 1: Binarization of the Output Response by Thresholding. The conditioned reflex circuit in Figure 2 was designed with the minimal structure required to meet the specifications. Depending on practical applications, appropriate mechanisms can be added to reprocess the output property of the conditioned reflex circuit. Following, we demonstrate a binarization of output response using a threshold gate that can distinguish between logically low and high in the output with reference to a threshold level. Let the threshold gate be connected to the conditioned reflex circuit as shown in Figure 6A, and observe the new output, Z. In this demonstration, we employed a seesaw gate[25] as a thresholding mechanism comprising thresholding ($r_{f_1}^{(T)}$ and $r_{b_1}^{(T)}$) and amplification mechanisms ($r_{f_2}^{(T)}$, $r_{b_2}^{(T)}$, $r_{f_3}^{(T)}$, and $r_{b_3}^{(T)}$) in Figure 6B. Since the conditioned reflex circuit must respond to repetitive inputs for learning, the seesaw gate is also required to be renewable. Here, we adopt a renewable design with the photoresponsive molecule, "azobenzene." A photoresponsive control design using the azobenzene modification of DNA strands can make DNA circuits renewable.[26,27] Azobenzene can exist in two structures, the trans and cis forms, which can be interconverted under ultraviolet (UV) and blue light (BL) irradiation, respectively.[28] When azobenzene is incorporated into the DNA base sequence, the stability of the double-helix structure can be controlled by light irradiation. Specifically, under BL irradiation, the trans form stabilizes the double-stranded structure, while under UV irradiation, the cis form destabilizes it. This property of azobenzene can be applied to DNA strand displacement reactions by modifying the toehold and recognition domains with azobenzene, which can alter the balance between forward and backward reaction flows by using BL/UV irradiation. In this demonstration, we performed photoresponsive control such that the thresholding executed the binarization of output responses from the conditioned reflex circuit under BL or was initialized toward the initial concentration under UV irradiation (Figure 6D). In accordance with the renewable design proposed by Tamba et al.,[27] domains s_2, $s_1't_b^*$, t_b^*, and s_2t_b of O, T_v, T_g, and T_f, respectively, were modified with azobenzene, where as much azobenzene as possible was inserted in these domains (Figure 6B,C). Under BL irradiation (in Figure 6B), all reactions ($r_{f_1}^{(T)}$, $r_{b_1}^{(T)}$, $r_{f_2}^{(T)}$, $r_{b_2}^{(T)}$, $r_{f_3}^{(T)}$, and $r_{b_3}^{(T)}$) occurred based on the usual strand displacement mechanism, meaning that the gate functioned as a threshold gate. For UV irradiation (Figure 6C), a set of reactions ($\overline{r}_{b_1}^{(T)}$, $\overline{r}_{b_2}^{(T)}$, and $\overline{r}_{f_4}^{(T)}$) became dominant, and as a consequence, all reactions of the threshold gate proceeded in the direction of the initial concentrations, indicating that the gate was initialized. Figure 6E shows the simulation results in

https://doi.org/10.1021/acssynbio.3c00459
ACS Synth. Biol. 2024, 13, 521−529

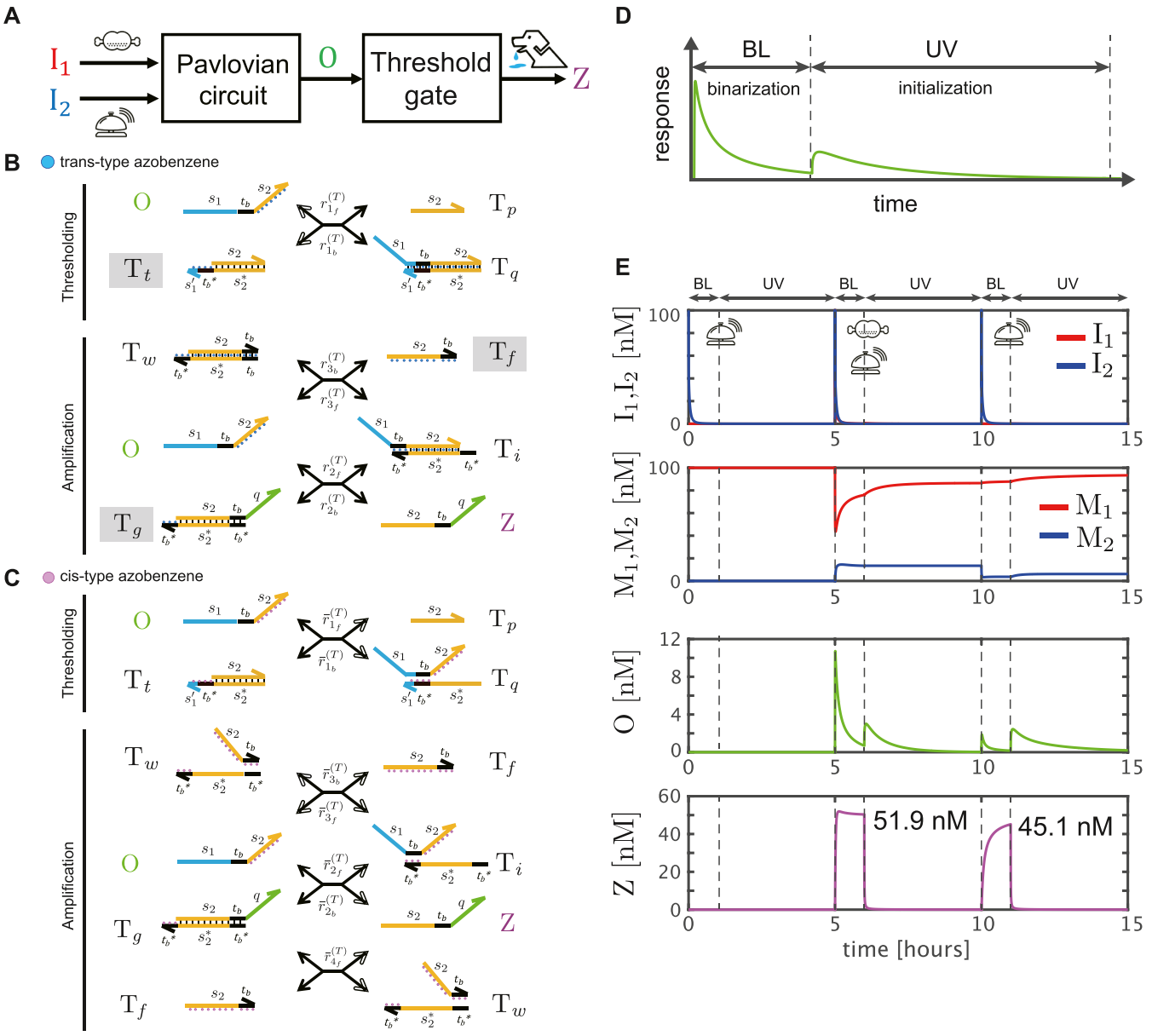

Figure 6. Binarization of output response by thresholding. (A) Threshold gate is connected to the conditioned reflex circuit. (B,C) Schematic views of the threshold gate under blue light (BL) irradiation (B) and ultraviolet (UV) irradiation (C) conditions, where the reactions are comprised of four single-stranded DNAs (O, T_p, T_f, and Z) and five double-stranded DNAs (T_t, T_q, T_g, T_i, and T_w) and are denoted by the bidirectional arrows connecting the DNA strands in the same notation as in Figure 2, except that considerably slow reactions are represented by white arrows. Small circles attached to domains denote azobenzene modifications, where blue ones in (B) and purple ones in (C) are *trans*- and *cis*-type azobenzene, respectively. Double-stranded DNAs with initial concentrations are denoted by shadowed, square boxes. Corresponding ordinary differential equations, the initial concentrations, and the reaction rates are described in Text S3. (D) Timing chart of the photoresponsive control. BL or UV was irradiated alternately. (E) First, second, third, and fourth panels show the time-course data of inputs, memory gates, net output of the conditioned reflex circuit, and binarized output of the threshold gate, respectively. The peak values of Z upon the "FB" and the second "B" inputs are denoted in the fourth panel.

the case of input patterns "B−FB−B", which satisfy the learning condition; the initial concentrations of the threshold gate were given by $[T_t](0) = [T_g](0) = [T_f](0) = 100$ nM (others 0), and irradiation durations were set at 1 and 4 h for BL and UV, respectively. The threshold gate enhanced the net output responses from the conditioned reflex circuit upon the "FB" and the second "B" inputs and was effective in logically distinguishing between high and low.

Discussion 2: Synchronization in Learning Conditions. It has been reported that the learning principle of Pavlovian conditioning in the brain revealed the importance of activation synchronization induced by unconditioned and conditioned stimuli within a narrow time window.[23] In our design, the condition for a memory gate M_2 to be updated is the simultaneous existence of the I_1-induced Y_2 strand and the I_2-induced W_2 strand, as shown in Figure S2C. Hence, as long as the time of the I_1 and I_2 inputs is within a time window, the learning condition is expected to be satisfied. As shown in Figure 7, the accumulated M_2 concentration decreased monotonically as the interval between the I_1 and I_2 inputs became longer. Consequently, the peak of the output response also had a similar profile as that of the interval. Therefore, our

https://doi.org/10.1021/acssynbio.3c00459
ACS Synth. Biol. 2024, 13, 521−529

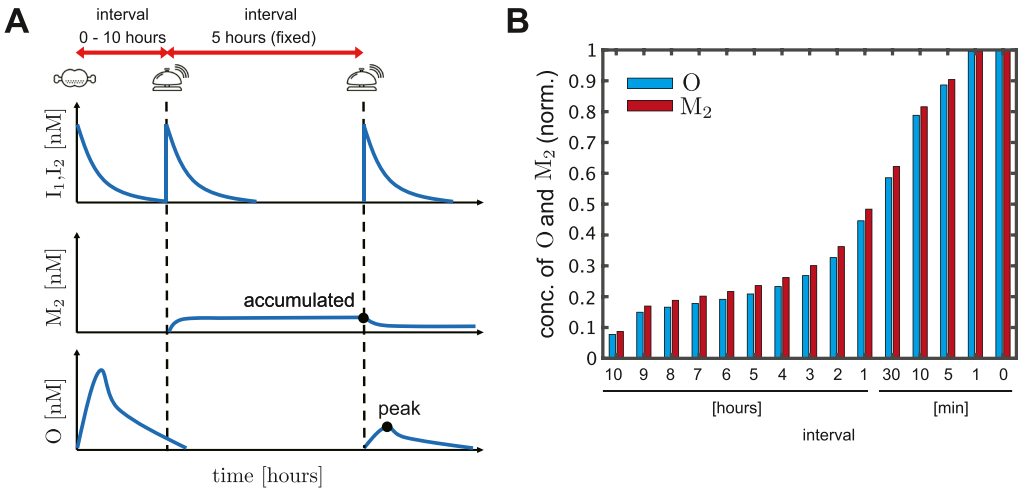

Figure 7. Synchronization in learning conditions (A) Interval between the first and second inputs of the input pattern "F−B−B" were changed from 0 to 10 h, where 0 min represents the simultaneous inputs of I_1 and I_2, and the interval between the second and third inputs was fixed at 5 h. The accumulated concentrations of M_2 after the second input and the peaks of output O after third input were investigated. (B) Simulation results of the accumulated M_2 concentrations and the peaks of the output O are shown by red- and blue-colored bars, respectively. The vertical axis is normalized by the concentrations in the simultaneous input case.

design reproduces the properties of synchronization in Pavlovian conditioning.

Discussion 3: Implications for Functional Enhancements. As can be seen, the conditioned reflex circuit consists of five DNA strand displacement reactions and two degradation reactions. Provided that the degradation reactions are also implemented by an enzyme-free mechanism, the entire circuit becomes a completely enzyme-free system. For example, an enzyme-free degradation mechanism based on DNA strand displacement reactions is available[29] and has been applied to various circuits.[27,30] As discussed in an earlier study,[7] enzyme-free designs allow us to analyze/design the reaction systems in detail and perform mathematical modeling based on the well-defined DNA strand displacement mechanism without black-box mechanisms. In addition, it would be beneficial to take the enzyme-free design in some situations such that the conditioned reflex circuit is connected to other enzyme-free circuits or experimental constraints (buffer composition, temperature, pH) are appropriate for an enzyme-free system.

However, if the entire reaction system, including the DNA strand displacement cascades, degradation reactions, and thresholding gates, can be reconstructed based on enzymatic reaction design such as PEN toolbox[31,32] while assuring renewability, it might be possible to enhance reaction speed and robustness and further simplify the circuit.[7,33]

Regarding the freedom of input channels of the conditioned reflex circuit, the generalized version of the circuit can receive multiple kinds of input strands but still requires prescribing the base sequence for each input strand. To deal with arbitrary input sequences rather than a preset of sequences, one might consider a polymerase-based primer exchange reaction to generate user-specified sequences from primer strands applied to the circuit.[34]

CONCLUSIONS

In this study, we explored the operating principle of biochemical reaction systems with intrinsic plastic adaptation capabilities and designed a DNA circuit that possesses classical conditioning. The designed circuit was simply constructed with a maximum of five DNA strand displacement reactions and two degradation reactions. Taking advantage of the dynamical properties in the DNA circuit based on the input history of the kind and timing, as suggested by the learning principles of the Pavlovian-conditioned reflex, provides freedom in DNA circuit design.

Our design sought to address the design issue in the simplest manner to improve further the performance, including the efficiency, robustness, and reliability of the learning system. However, according to the required specifications for an application, incorporation of various technical ingenuities from the sequence, molecular, and platform levels is needed, such as the introduction of clamp domains,[25] artificial nucleic acids,[35] or enzymatic reaction mechanisms, including the PEN DNA toolbox[31] and the BIO-PC system.[36]

If considering a direct application in future studies, the conditioned reflex circuit designed herein provides a logic circuit in which the YES and OR functions are switched reversibly according to the input condition. For example, by creating a tree-structured network by connecting the two-input and one-output YES/OR switching circuits in a modular manner, it is proposed that more intelligent circuits will be designed that are capable of acquiring various functions by learning.[37]

METHODS

The mathematical model of the conditioned reflex circuit shown in Figure 2 is given by ordinary differential equations based on chemical kinetics (Text S1). All reaction rates and the initial concentrations of the conditioned reflex circuit were estimated as follows.

Let the peak and steady-state values of the output response induced by the simultaneous I_1 and I_2 inputs be represented by $J_{pk}^{(1,2)}$ and $J_{ss}^{(1,2)}$. Similarly, the peak and steady-state values of the output response induced by the I_2 input are represented by $J_{pk}^{(2)}$ and $J_{ss}^{(2)}$. Following the specifications of the conditioned reflex circuit defined in the "Circuit design" section, we consider the output responses induced by the simultaneous I_1 and I_2 inputs at the prelearning condition and the I_2 input at the postlearning condition, as shown in Figure S14. The cost

https://doi.org/10.1021/acssynbio.3c00459
ACS Synth. Biol. 2024, 13, 521−529

function employed for the parameter estimation of the conditioned reflex circuit is designed by

$$J(x(0), p) = \frac{\alpha_1}{J_{pk}^{(1,2)}} + \alpha_2 J_{ss}^{(1,2)} + \frac{\alpha_3}{J_{pk}^{(2)}} + \alpha_4 J_{ss}^{(2)} \quad (1)$$

where $x(0)$ is the initial concentration vector and $p = [k_{1_f}^{(1)} k_{1_b}^{(1)} k_{1_f}^{(2)} k_{1_b}^{(2)} \overline{k}_{1_f}^{(2)} \overline{k}_{1_b}^{(2)} k_{2_f}^{(1)} k_{2_b}^{(1)} k_{2_f}^{(2)} k_{2_b}^{(2)} k_d^{(1)} k_d^{(2)}]^T$ is the parameter vector comprising reaction rates (also see Text S1). The nonlinear optimization problem of parameter estimation is then formulated as follows: Minimize the cost function J subject to the initial concentration $x(0)$ and the kinetic parameter p. Generally, the reaction rates depend on the toehold lengths involved in a strand displacement reaction and the reaction temperature and, therefore, have distinct values depending on these conditions. Hence, when evaluating the cost function, the lengths of toeholds t_1, t_2, t_a, and t_b were searched in the range of 3−6, respectively, and p was calculated according to the calculation method,[38] where 100 nM inputs are applied to the circuit, lengths of the recognition domains a_1, a_2, s_1, and s_2 are fixed by 20 nt, and temperature is assumed to be 37 °C. We successfully determined that the optimal initial concentrations were $[M_1](0) = [M_{2p}](0) = [S](0) = [R_2](0) = 100$ nM, $[R_1](0) = 50$ nM, and the others were 0 nM; the degradation rates were $k_d^{(1)} = k_d^{(2)} = 0.01$ 1/s, and the optimal lengths of toeholds t_1, t_2, t_a, and t_b were 5 nt, where the "ga" (genetic algorithm) library of Global Optimization Toolbox in Matlab was used, and the estimated values were rounded to one significant digit. Then, all strand displacement reaction rates, $k_{i_f}^{(j)}$, $k_{i_b}^{(j)}$, $\overline{k}_{1_f}^{(1)}$, and $\overline{k}_{1_b}^{(1)}$ $(i, j = 1, 2)$ were calculated as 5.32×10^{-4} 1/nMs with 164 nM in the critical concentration. The validity of the estimated parameter values was further evaluated by using the sensitivity analysis in Text S4. The mathematical model of the generalized conditioned reflex circuit shown in Figure 5 is also given in Text S2.

■ ASSOCIATED CONTENT

Supporting Information

The Supporting Information is available free of charge at https://pubs.acs.org/doi/10.1021/acssynbio.3c00459.

Figures regarding the conditioned reflex circuit drawn by Visual DSD, operating and learning principles, simulations of the acquisition and forgetting of conditioned reflexes under different conditions, simulations of the generalized conditioned reflex circuit, the cost function of the parameter estimation, mathematical modeling of the (generalized) conditioned reflex circuit and the renewable threshold gate, and description of optimization of learning efficiency (PDF)

■ AUTHOR INFORMATION

Corresponding Author

Takashi Nakakuki − *Department of Intelligent and Control Systems, Faculty of Computer Science and Systems Engineering, Kyushu Institute of Technology, Fukuoka 8208502, Japan;* orcid.org/0000-0003-0973-4177; Phone: +81 (0)948 297716; Email: nakakuki@ics.kyutech.ac.jp

Authors

Masato Toyonari − *Department of Intelligent and Control Systems, Faculty of Computer Science and Systems Engineering, Kyushu Institute of Technology, Fukuoka 8208502, Japan*

Kaori Aso − *Department of Intelligent and Control Systems, Faculty of Computer Science and Systems Engineering, Kyushu Institute of Technology, Fukuoka 8208502, Japan*

Keiji Murayama − *Department of Biomolecular Engineering, Graduate School of Engineering, Nagoya University, Nagoya 4648603, Japan;* orcid.org/0000-0002-6537-0120

Hiroyuki Asanuma − *Department of Biomolecular Engineering, Graduate School of Engineering, Nagoya University, Nagoya 4648603, Japan;* orcid.org/0000-0001-9903-7847

Tom F. A. de Greef − *Laboratory of Chemical Biology and Institute for Complex Molecular Systems and Computational Biology Group, Department of Biomedical Engineering, Eindhoven University of Technology, Eindhoven 5600 MB, The Netherlands;* orcid.org/0000-0002-9338-284X

Complete contact information is available at: https://pubs.acs.org/10.1021/acssynbio.3c00459

Author Contributions

TN conceived of the study. TN, KA, and TG designed the reaction schemes. TN, KM, and HA designed the azobenzene-based mechanism. TN and MT performed the simulations and the sensitivity analysis. TN wrote the manuscript.

Notes

The authors declare no competing financial interest.

■ ACKNOWLEDGMENTS

This work was supported by JSPS KAKENHI Grant Numbers 20KK0331 (T.N.), 20H05971 (T.N.), 20K04549 (T.N.), 23H00506 (T.N.), 20H05970 (K.M.), 20H05968 (K.M.), and JP21H05025 (H.A.).

■ REFERENCES

(1) Shinar, G.; Feinberg, M. Structural sources of robustness in biochemical reaction networks. *Science* **2010**, *327*, 1389−1391.

(2) Araujo, R. P.; Liotta, L. A. Universal structures for adaptation in biochemical reaction networks. *Nat. Commun.* **2023**, *14*, 2251.

(3) Alon, U. *An Introduction to Systems Biology: Design Principles of Biological Circuits*; Taylor & Francis, 2006.

(4) Huse, M.; Kuriyan, J. The conformational plasticity of protein kinases. *Cell* **2002**, *109*, 275−282.

(5) Dueber, J. E.; Yeh, B. J.; Bhattacharyya, R. P.; Lim, W. A. Rewiring cell signaling: the logic and plasticity of eukaryotic protein circuitry. *Curr. Opin. Struct. Biol.* **2004**, *14*, 690−699.

(6) Whitacre, J. M. Biological robustness: paradigms, mechanisms, and systems principles. *Front. Genet.* **2012**, *3*, 67.

(7) Srinivas, N.; Parkin, J.; Seelig, G.; Winfree, E.; Soloveichik, D. Enzyme-free nucleic acid dynamical systems. *Science* **2017**, *358*, No. eaal2052.

(8) Lakin, M. R.; Stefanovic, D. Supervised Learning in Adaptive DNA Strand Displacement Networks. *ACS Synth. Biol.* **2016**, *5*, 885−897.

(9) Cherry, K. M.; Qian, L. Scaling up molecular pattern recognition with DNA-based winner-take-all neural networks. *Nature* **2018**, *559*, 370−376.

(10) Zou, C.; Wei, X.; Zhang, Q.; Zhou, C. A Novel Adaptive Linear Neuron Based on DNA Strand Displacement Reaction Network. *IEEE/ACM Trans. Comput. Biol. Bioinf.* **2020**, *19*, 1424−1434.

(11) Zou, C.; Zhang, Q.; Zhou, C.; Cao, W. A nonlinear neural network based on an analog DNA toehold mediated strand displacement reaction circuit. *Nanoscale* **2022**, *14*, 6585−6599.
(12) Qian, L.; Winfree, E.; Bruck, J. Neural network computation with DNA strand displacement cascades. *Nature* **2011**, *475*, 368−372.
(13) Kieffer, C.; Genot, A. J.; Rondelez, Y.; Gines, G. Molecular Computation for Molecular Classification. *Adv. Biol.* **2023**, *7*, No. e2200203.
(14) Lakin, M.; Stefanovic, D. Towards Temporal Logic Computation Using DNA Strand Displacement Reactions; Patitz, M.; Stannett, M., Eds. In *Unconventional Computation and Natural Computation. UCNC 2017. Lecture Notes in Computer Science*, 2017; Vol *10240*
(15) Lapteva, A. P.; Sarraf, N.; Qian, L. DNA Strand-Displacement Temporal Logic Circuits. *J. Am. Chem. Soc.* **2022**, *144*, 12443−12449.
(16) Hsiao, V.; Hori, Y.; Rothemund, P. W.; Murray, R. M. A population-based temporal logic gate for timing and recording chemical events. *Mol. Syst. Biol.* **2016**, *12*, 869.
(17) O'Brien, J.; Murugan, A. Temporal Pattern Recognition through Analog Molecular Computation. *ACS Synth. Biol.* **2019**, *8*, 826−832.
(18) Zhang, M.; Sun, Y. DNA-based customized functional modules for signal transformation. *Front Chem.* **2023**, *11*, 1140022.
(19) Zhao, S.; Liu, Y.; Zhang, X.; Qin, R.; Wang, B.; Zhang, Q. Mapping Temporally Ordered Inputs to Binary Message Outputs with a DNA Temporal Logic Circuit. *Nanomaterials* **2023**, *13*, 903.
(20) Bucci, J.; Irmisch, P.; Del Grosso, E.; Seidel, R.; Ricci, F. Orthogonal Enzyme-Driven Timers for DNA Strand Displacement Reactions. *J. Am. Chem. Soc.* **2022**, *144*, 19791−19798.
(21) Murata, S.; Toyota, T.; Nomura, S.-i. M.; Nakakuki, T.; Kuzuya, A. Molecular Cybernetics: Challenges toward Cellular Chemical Artificial Intelligence. *Adv. Funct. Mater.* **2022**, *32*, 2201866.
(22) Pavlov, I. P. Conditioned reflexes: An investigation of the physiological activity of the cerebral cortex. *Ann. Neurosci.* **2010**, *17*, 136.
(23) Yagishita, S.; Hayashi-Takagi, A.; Ellis-Davies, G. C. R.; Urakubo, H.; Ishii, S.; Kasai, H. A critical time window for dopamine actions on the structural plasticity of dendritic spines. *Science* **2014**, *345*, 1616−1620.
(24) Lakin, M. R.; Youssef, S.; Polo, F.; Emmott, S.; Phillips, A. Visual DSD: a design and analysis tool for DNA strand displacement systems. *Bioinformatics* **2011**, *27*, 3211−3213.
(25) Qian, L.; Winfree, E. Scaling up digital circuit computation with DNA strand displacement cascades. *Science* **2011**, *332*, 1196−1201.
(26) Song, X.; Eshra, A.; Dwyer, C.; Reif, J. Renewable DNA seesaw logic circuits enabled by photoregulation of toehold-mediated strand displacement. *RSC Adv.* **2017**, *7*, 28130−28144.
(27) Tamba, M.; Murayama, K.; Asanuma, H.; Nakakuki, T. Renewable DNA Proportional-Integral Controller with Photoresponsive Molecules. *Micromachines* **2022**, *13*, 193.
(28) Asanuma, H.; Liang, X.; Nishioka, H.; Matsunaga, D.; Liu, M.; Komiyama, M. Synthesis of azobenzene-tethered DNA for reversible photo-regulation of DNA functions: hybridization and transcription. *Nat. Protoc.* **2007**, *2*, 203−212.
(29) Oishi, K.; Klavins, E. Biomolecular implementation of linear I/O systems. *IEE Proc.: Syst. Biol.* **2011**, *5*, 252−260.
(30) Yordanov, B.; Kim, J.; Petersen, R. L.; Shudy, A.; Kulkarni, V. V.; Phillips, A. Computational design of nucleic acid feedback control circuits. *ACS Synth. Biol.* **2014**, *3*, 600−616.
(31) Montagne, K.; Plasson, R.; Sakai, Y.; Fujii, T.; Rondelez, Y. Programming an in vitro DNA oscillator using a molecular networking strategy. *Mol. Syst. Biol.* **2011**, *7*, 466.
(32) Montagne, K.; Gines, G.; Fujii, T.; Rondelez, Y. Boosting functionality of synthetic DNA circuits with tailored deactivation. *Nat. Commun.* **2016**, *7*, 13474.
(33) Okumura, S.; Gines, G.; Lobato-Dauzier, N.; Baccouche, A.; Deteix, R.; Fujii, T.; Rondelez, Y.; Genot, A. J. Nonlinear decision-making with enzymatic neural networks. *Nature* **2022**, *610*, 496−501.
(34) Kishi, J. Y.; Schaus, T. E.; Gopalkrishnan, N.; Xuan, F.; Yin, P. Programmable autonomous synthesis of single-stranded DNA. *Nat. Chem.* **2018**, *10*, 155−164.
(35) Chen, Y.; Nagao, R.; Murayama, K.; Asanuma, H. Orthogonal Amplification Circuits Composed of Acyclic Nucleic Acids Enable RNA Detection. *J. Am. Chem. Soc.* **2022**, *144*, 5887−5892.
(36) Joesaar, A.; Yang, S.; Bögels, B.; van der Linden, A.; Pieters, P.; Kumar, B. V. V. S. P.; Dalchau, N.; Phillips, A.; Mann, S.; de Greef, T. F. A. DNA-based communication in populations of synthetic protocells. *Nat. Nanotechnol.* **2019**, *14*, 369−378.
(37) Azuma, S.-i.; Takakura, D.; Ariizumi, R.; Asai, T. Networks of Classical Conditioning Gates and Their Learning. *arXiv* **2023**, arXiv:2312.15161.
(38) Zhang, D. Y.; Winfree, E. Control of DNA strand displacement kinetics using toehold exchange. *J. Am. Chem. Soc.* **2009**, *131*, 17303−17314.

https://doi.org/10.1021/acssynbio.3c00459
ACS Synth. Biol. 2024, 13, 521−529